AIP Physics of Fluids

Segregation time-scale in bi-disperse granular flows

L. Staron and J. C. Phillips

Citation: Physics of Fluids (1994-present) **26**, 033302 (2014); doi: 10.1063/1.4867253
View online: http://dx.doi.org/10.1063/1.4867253
View Table of Contents: http://scitation.aip.org/content/aip/journal/pof2/26/3?ver=pdfcov
Published by the AIP Publishing

PHYSICS OF FLUIDS **26**, 033302 (2014)

Segregation time-scale in bi-disperse granular flows

L. Staron[1,2] and J. C. Phillips[2]
[1]*Sorbonne Universités, UPMC Univ Paris 06, CNRS, UMR 7190, Institut Jean Le Rond d'Alembert, F-75005 Paris, France*
[2]*School of Earth Sciences, University of Bristol, Bristol, United Kingdom*

(Received 9 May 2013; accepted 12 February 2014; published online 6 March 2014)

Using a discrete simulation method, we investigate numerically two-dimensional bi-disperse chute flows formed of a layer of larger grains overlaid by a layer of smaller grains, and analyze their evolution for different slopes and different volume fraction of large beads. As size segregation occurs, the vertical position of the centre of mass of the large beads is shown to increase exponentially with time with a typical time scale decreasing with their volume fraction. A simple model balancing lift and drag forces acting on large particles recovers this dynamics, successfully predicts the typical time scale of segregation, and permits to relate this typical time scale to the flow dynamics. © *2014 AIP Publishing LLC*. [http://dx.doi.org/10.1063/1.4867253]

I. INTRODUCTION

Size segregation in granular systems is a frequent phenomenon easily observed once the distribution of grains sizes is sufficiently large, and the system undergoes a sufficiently rapid, or long-lasting, shear motion. In this situation, larger grains raise to the surface while smaller ones sink to the bottom as a result of "kinematic sieving," leading to heterogeneous patterns and spatial ordering.[1,2] Its occurrence is relevant to a wide variety of contexts. In industrial applications handling raw material in the shape of grains, or pharmaceutical processes handling powders with different properties, segregation forms a serious obstacle to efficient mixing, and a long-lasting issue for engineers. In geological processes, where the sorting of grains by size in deposits—river beds,[3,4] volcanic flows,[5,6] debris, and rock avalanches for instance[7]—contains the signature of the systems dynamics, the mechanisms dominating segregation are a key element towards better understanding of the geophysical processes. An improved physical characterization of the physics of grain size segregation is thus a highly desirable scientific objective.

However, in spite of its generic interest, and the facility with which the phenomenon can be observed, this characterization remains lacking due to many difficulties. First, simple mono-disperse granular beds are already complex systems: the puzzles they have consistently opposed to scientific investigation are necessarily present in the case of bi- or poly-disperse systems. This includes the difficulty of accessing dynamical quantities (stresses and velocities) experimentally. Precise and fundamental insight was gained from the study of a single intruder in a mono-disperse packing;[8] however, generic segregation is a collective phenomena. The relevance of a single intruder's behavior to many large grains flowing in a matrix of smaller ones is not entirely clear. Finally, segregation is by essence a transient phenomenon. It starts as a result of shear when large grains are at the bottom, and stops when they have risen to the top; meanwhile, the local volume fraction of large and small grains varies in space and time, and the shear rate is likely to vary locally accordingly. Relating the force allowing large grains to rise to the system's state and dynamics is thus uneasy.

However, steady progress has been made using a combination of experimental, numerical, and theoretical approaches.[9–17] It was shown for instance that the rheological properties of bi-disperse flows fall in the same framework as mono-disperse flows, although the actual quantitative effects of segregation on flow mobility (or frictional properties) was not unambiguously established.[18–22] In this respect, it can be noted that the difference between three-dimensional and two-dimensional dynamics is of fundamental significance, segregation inducing the formation of patterns in the system: channelizing, layering, thus adding difficulty to the understanding of the problem.[5,7,23,24] With respect to modeling, much progress has been made using shallow-layer approximations for bi-phasic flows incorporating an effective separating force induced by partial pressures and a viscous drag force,[9,25] allowing for the recovery of various experimental observations.[7,24,26] In this context, an explicit relation between segregation rate, segregation velocity, and the flow dynamics would be of interest.

In the present study, we are interested in characterizing the rise of the larger beads as a result of the flow dynamics, and in understanding what controls the efficiency of the mechanism, i.e., the typical time scale of segregation. To this purpose, discrete numerical simulation is a helpful tool, first because it allows for perfectly well-controlled "experimental" conditions (contact properties, flow geometry, flow duration), but mostly because it provides direct knowledge of the state of the system (velocities, forces, volume fraction).

Simulating two-dimensional bi-disperse chute flows formed of larger and smaller grains, we analyze their evolution for different slopes and different volume fraction of large grains. As size segregation occurs, the mean vertical position of the large grains is shown to rise exponentially with time with a typical time scale decreasing with their volume fraction. A simple model balancing effective lift and drag forces leads to the recovery of this dynamics, yields successful prediction for the typical time scale of segregation, and allows for relating the latter to the flow dynamics. The results are discussed in relation to existing theoretical modeling of the segregation mechanism and previous experimental studies of the segregation time-scale.[9,11]

II. THE NUMERICAL FLOWS

The numerical experiment is in its principle similar to those reported in previous studies:[20,27] a granular free surface flow over an incline allowing for steady flow regimes involving different grain sizes. In this contribution, we adopt a perfectly two-dimensional geometry; we consider a granular layer made of two species of grains of circular shape, on an incline of slope θ, and subjected to gravity. The contact dynamics algorithm was applied.[28] By contrast with discrete element methods (DEM) methods (used, for instance, in Refs. 20 and 27), the contact dynamics method does not prescribe an explicit mathematical form for the contact force between the grains, but takes into account the rigidity of the grains and the existence of a friction threshold through the introduction of discontinuities for velocities and forces in the mathematical solver. Perfectly rigid grains are thus assumed. They interact at contact through solid friction: locally, the normal and tangential contact forces satisfy $f_t \leq \mu f_n$, where μ is the coefficient of friction at contact. Moreover, a coefficient of energy restitution e set the amount of energy dissipated in collisions. The numerical values of μ and e control the effective frictional properties of the flow in a given configuration. They are strictly the same for all contacts between large and small grains. In the present work, we are not interested in understanding how they may affect the segregation process, hence, their value was set to $\mu = 0.5$ and $e = 0.25$, and were not varied. The value $e = 0.25$ is a low coefficient of restitution and coincides with a dense packing. Note however that as long as $e < 0.8$, the dynamics of the flow is marginally affected, collisions remaining very efficient at dissipating energy. Choosing $e \to 1$ would induce a bouncing dynamics dominated by binary collisions; this however is not a case we are interested in at present. Importantly, the value of e does not affect the accuracy of the computation by the contact dynamics algorithm, which considers non-smooth contact interactions.

Figure 1 shows a typical system. The large beads have a mean diameter d_L and the small beads have a mean diameter d_S. To prevent geometrical ordering, likely to happen in 2D for strictly mono-sized packings, both large and small grains have diameters uniformly distributed around their mean value: if we denote $d_L^{\min}$ and $d_L^{\max}$ (respectively, $d_S^{\min}$ and $d_S^{\max}$) the lower and upper bounds of the size distribution of large grains (respectively, the size distribution of small grains), we chose $\Delta = \frac{(d_L^{\max} - d_L^{\min})}{d_L} = \frac{(d_S^{\max} - d_S^{\min})}{d_S} = 0.4$ in most of the simulations presented here; thus, the systems are not strictly bi-disperse. The effect of the dispersion Δ of grains sizes around their mean value on the degree of segregation was systematically investigated. The ratio d_L/d_S was not varied, and we chose $d_L/d_S = 2$.

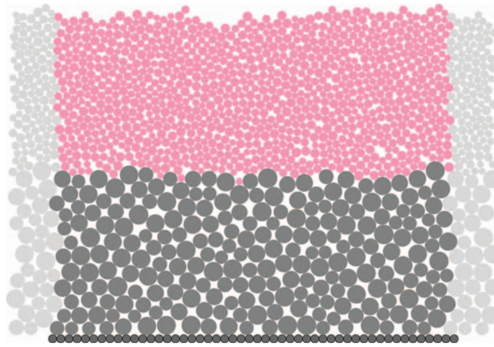

FIG. 1. A periodic bi-disperse granular bed in its initial state: a layer of large grains is overlaid by a layer of small grains.

To ensure long flow durations, periodic boundary conditions were implemented; the width of the simulation cell is $50d_S$. The basal boundary is made of a row of fixed beads of diameter d_S. In the initial state, a layer of large beads is overlaid by a layer of small beads. This is achieved by random deposition under gravity. We denote ξ the volume fraction of large beads, i.e., the ratio of the volume of large beads to the total volume of grains: $\xi = V_L/(V_S + V_L)$. Accordingly, the volume fraction of small beads is given by $(1 - \xi)$. In the simulations, ξ was varied between 0.08 and 0.89; accordingly the number of grains varies between 900 and 2000. The height of the granular bed in the initial state is H. Irrespective of ξ, H was kept constant and equal to $H \simeq 45d_S$ (later when the flow develops, the height of the flow may vary slightly as a result of both shear motion and segregation). The initial height of large beads is thus ξH, and the initial height of small beads is thus $(1 - \xi)H$. The slope of the granular bed θ was varied between 17.5° and 22° to the horizontal, allowing different flow velocities.

The numerical values used for the simulations are the following: $d_S = 5 \times 10^{-3}$ m, $\rho = 1$ kg m^{-2}, $g = 9.8$ m s^{-2}. Table I shows a summary of all runs performed with varying volume fraction of large grains ξ, slope angle θ, and grain size distribution's width Δ.

III. AN EXPONENTIAL EVOLUTION

Figure 2 shows four successive snapshots of a flow with slope $\theta = 18°$ and $\xi = 0.37$: initial state, two intermediate stages, and final (stationary) state. As was observed in Refs. 20 and 27, the segregated state is characterized by a pure layer of large grains at the top, a pure layer of small grains at the bottom, and a large intermediate bi-disperse layer. We compute the vertical position of the centre of mass of the large beads y_G:

$$y_G = \frac{1}{n_L}\sum_{i=1}^{n_L} y_i,$$

TABLE I. Table of simulations performed.

Simulations set	Volume fraction of large beads ξ	Slope θ	Grain size distribution width Δ	Number of runs n
Set 1	$0.08 \leq \ldots \leq 0.93$	18°	0.4	55
Set 2	0.5	18°	$0.08 \leq \ldots \leq 0.32$	4
Set 3	0.16	$17.5° \leq \ldots \leq 22°$	0.4	15
Set 4	0.34	$17.5° \leq \ldots \leq 22°$	0.4	15
Set 5	0.5	$17.5° \leq \ldots \leq 22°$	0.4	15
Set 6	0.67	$17.5° \leq \ldots \leq 22°$	0.4	15

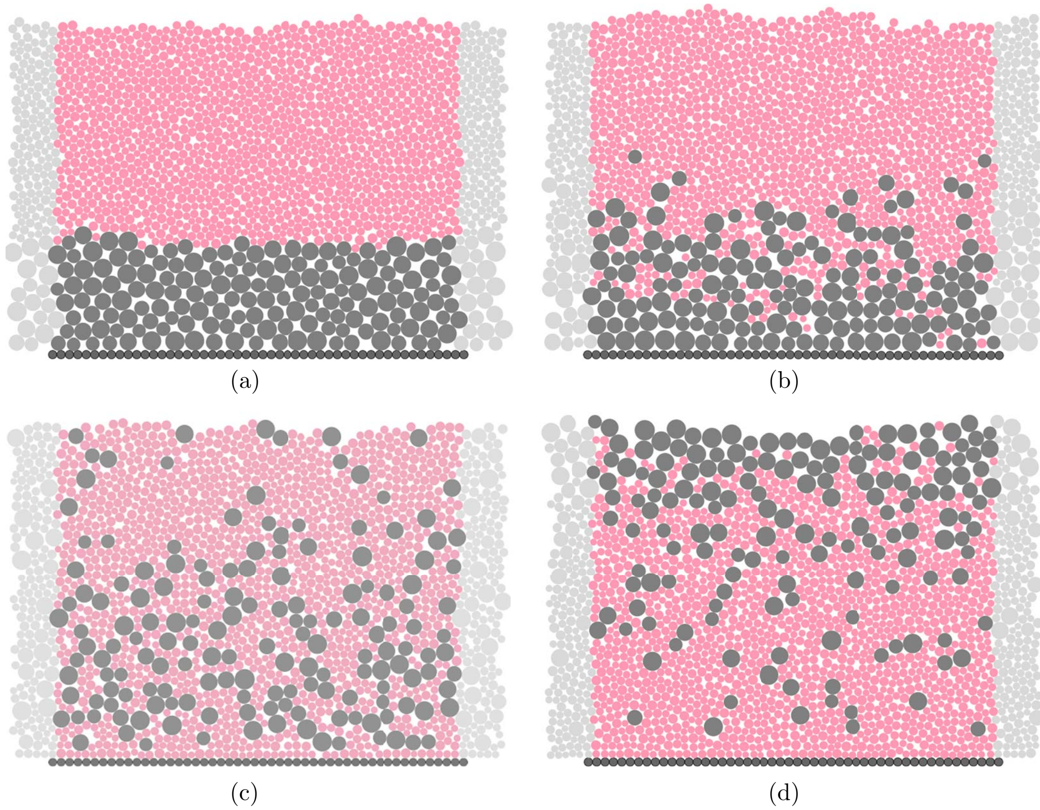

FIG. 2. Four snapshots of the segregation process in a granular flow of slope $\theta = 18^\circ$ with a volume fraction of large beads $\xi = 0.37$, from initial to steady state.

where n_L is the total number of large grains, and y_i is the vertical position of the grain i. For the example shown in Figure 2, y_G is plotted as a function of time in Figure 3: it exhibits an exponential increase towards a saturated segregated state which corresponds to the stationary regime.

The exponential rise of the large beads in the flow is a robust feature: the position of the centre of mass of the large grains y_G obeys the following evolution:

$$y_G(t) = y_0 + (y_\infty - y_0)\left(1 - \exp(-\frac{t}{\tau})\right), \tag{1}$$

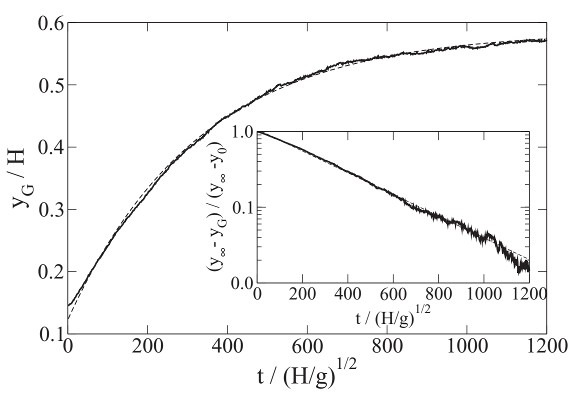

FIG. 3. Position y_G of the centre of mass of the large beads (normalized by the flow height H) as a function of time t (normalized by $\sqrt{H/g}$) for a granular flow of slope $\theta = 18^\circ$ and volume fraction of large beads $\xi = 0.37$. The dotted line shows the exponential fit. Inset graph: same evolution with respect to initial and final position $(y_\infty - y_G)/(y_\infty - y_0)$ in a log-lin graph.

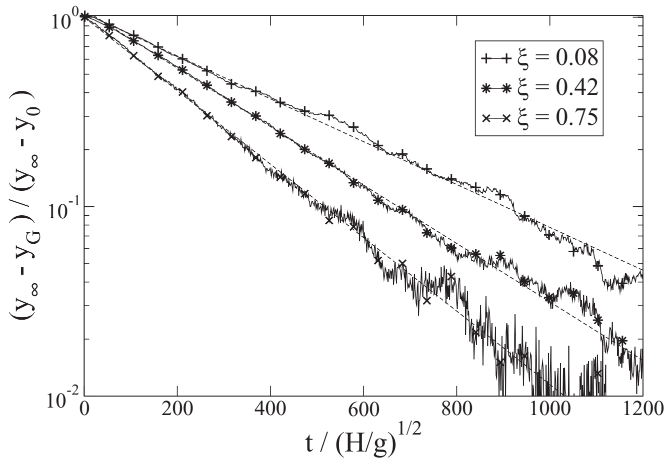

FIG. 4. For $\theta = 18°$ and different values of ξ, $(y_\infty - y_G(t))/(y_\infty - y_0)$ is plotted as a function of time (normalized by $\sqrt{H/g}$) in a log-lin representation. The different slopes of the exponential fits (dotted lines) show a typical time τ decreasing with increasing ξ.

where y_0 and y_∞ are, respectively, the initial and final value of y_G, and τ is the typical time scale characterizing the segregation process. Plotting $(y_\infty - y_G(t))/(y_\infty - y_0)$ as a function of time in a log-lin representation for $\theta = 18°$ and $\xi = 0.08$, $\xi = 0.42$, and $\xi = 0.75$ (series 1 of simulations, Table I), we observe that the typical time τ decreases with increasing ξ (Figure 4): for large ξ, large grains go through a thinner layer of small grains, resulting in smaller raising times.

If segregation was complete, all large grains would go through the whole layer of small grains, and we would observe $y_\infty - y_0 = (1 - \xi)H$. From both Figures 2 and 3, however, it is apparent that the segregation process saturates: not every large grain rises through the layer of small grains, and we observe

$$y_\infty - y_0 = \alpha(1 - \xi)H \ , \ \ \alpha < 1.$$

Interestingly, the numerical value of the final degree of segregation α is not dependent on ξ, nor on the slope θ: varying ξ for $\theta = 18°$ (series 1 of simulation, Table I) or varying θ for $\xi = 0.34$ and $\xi = 0.67$ (series 4 and 6 of simulations, Table I), we find $\alpha \simeq 0.789$ (Figure 5). We conclude from this observation that the final degree of segregation is not affected by the flow dynamics in the range of slopes investigated here, nor it is affected by the composition of the flow.

Among the factors that may influence the value of α which are not investigated in this paper is the ratio of the grain sizes d_L/d_S. We may expect a larger ratio to increase the level of segregation, although the role of d_L/d_S was shown to be non-monotonous and more complex than suggested by intuition.[11,22,27] In the present contribution, $d_L/d_S = 2$ and the dependence of the system behavior on this value is not investigated. However, both large and small grains exhibit a size distribution of width Δ around the mean values d_L and d_S. The results discussed so far were obtained for $\Delta = 0.4$. It is worth assessing the influence of Δ on the segregation dynamics. Therefore, we consider narrower distributions: $\Delta = 0.32$, $\Delta = 0.24$, $\Delta = 0.16$, and $\Delta = 0.08$, in the case $\xi = 0.5$ and $\theta = 18°$ (series 2 of simulations, Table I). The corresponding data are reported in Figure 5: we observe that decreasing Δ, that is narrowing the grain size distribution for each grain species, induces a higher degree of segregation, i.e., enhances the efficiency of segregation mechanisms.

IV. A LIFT-AND-DRAG MODEL

Size segregation and the raising of the larger grains to the surface of the flow can be understood as resulting from kinematic sieving: while the layer is sheared, spaces open into which smaller grains have a higher probability to fall, gradually forcing the larger grains to rise. Although this picture conveys a clear and certainly faithful picture of how segregation proceeds, it tells us little about the

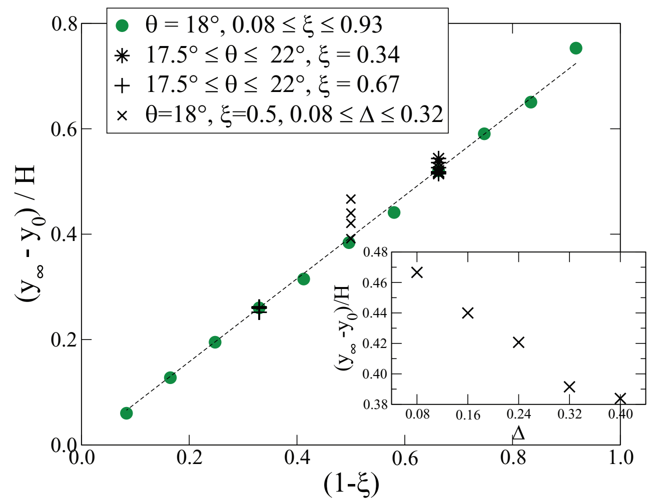

FIG. 5. Final displacement of the centre of mass of the large beads during the segregation process $y_\infty - y_0$ normalized by the flow height as a function of the volume fraction of small grains $(1 - \xi)$ for different slopes θ, compositions ξ, and grain size dispersion Δ. The effect of grain size dispersion Δ is specifically displayed in the inset. The dotted line shows a linear fit with slope 0.789.

actual upwards force applied to the larger grains. In Ref. 9, it is assumed that the smaller grains, as they fall through the matrix of larger ones, are partly screened from the mean stress applied to the system, which as a result is mostly supported by large grains. This departure from a homogenous pressure field creates effectively an upward motion of the large grains and downward motion of the smaller grains, without resorting to an explicit lift force. The idea is appealing; it was indeed shown that the mechanical strength of a poly-disperse packing is mainly sustained by the larger grains.[29] However, the computation of partial (computed over the whole volume of the flow) or intrinsic (computed over the volume occupied by each species) pressure in discrete simulations is unlikely to reflect more than either the volume fraction ratio, or the grain size ratio, as a straightforward consequence of the stress tensor expressions, unless the difference in the amplitude of the forces transmitted by each species is unreasonably large.

While the larger grains rise in the flow, the computation of the force resultant may provide an insight in the lift action they are submitted to. However, this signature is extremely noisy—grains rising intermittently, competing in the process, and exhibiting large fluctuations in their behavior—hence difficult to interpret in terms of effective lift and/or drag forces.

We seem thus to have little information on the forces seen altogether by the large rising grains, beside the observation that shear rate is a strong control on segregation. Nevertheless, there are simple assumptions one can make on the mechanism driving the large grains upwards. Assuming the existence of an effective lift force, it will depend on the degree of mixing of the bi-disperse mixture; it will be maximum when all the large grains lie at the bottom, but will tend to zero as they all rise at the surface. The degree of mixing is quantified by the position of the centre of mass of the large beads respective to its initial and final positions. Hence, a possible form for the lift force is

$$F_{\mathrm{lift}} = C \ \frac{y_\infty - y_G}{y_\infty - y_0}, \tag{2}$$

where C is a function with the following dimension: $[C] = \rho L^3 T^{-2}$ in a two-dimensional problem. We do not know *a priori* the form of C, beyond the fact that it is expected to depend on the shear rate (and on the size ratio between the grains, but this aspect is not investigated in this study). Note that although we use the terminology *lift* classically referring to Bernoulli effects, we do not imply any analogy between the effective segregation lift force discussed here and the former.

Due to the segregation lift force F_{lift}, the large grains rise in the flow through the layer of small grains at an average rate which can be described by the velocity of the centre of mass of the large beads $\dot{y}_G(t)$. As a result, the large grains experience an effective drag applied by the smaller grains. By analogy with the drag in viscous fluids, and in agreement with experimental studies on the form of drag forces in fluidized granular media,[30–32] the mean vertical velocity of the flow being zero, the drag force is given by

$$F_{\rm drag} = D\ \dot{y}_G, \tag{3}$$

where D is a function with the following dimension $[D] = \rho L^2 \cdot T^{-1}$ in a two-dimensional problem; again, we do not know *a priori* the form of D.

Finally, both large and small grains having the same density, and forming packings of identical packing fraction, no buoyant forces due to density gradients are active. Assuming that the vertical acceleration experienced by the large grains is negligible, the force balance is simply given by

$$F_{\rm lift} - F_{\rm drag} = 0, \tag{4}$$

$$C\ \frac{y_\infty - y_G}{y_\infty - y_0} - D\ \dot{y}_G = 0, \tag{5}$$

which can be rearranged into

$$\dot{y}_G + \frac{C}{D(y_\infty - y_0)} y_G - \frac{C y_\infty}{D(y_\infty - y_0)} = 0. \tag{6}$$

A straightforward solution to this differential equation is

$$y_G(t) = y_0 + (y_\infty - y_0)\left(1 - \exp(-\frac{C}{D(y_\infty - y_0)} t)\right). \tag{7}$$

The model thus recovers the behavior exhibited by the simulations.

Following this formulation, the typical time scale τ characterizing segregation depends on both lift and drag functions C and D, and on the trajectory of the center of mass of the large grains $y_\infty - y_0$. The model yields

$$\tau = \frac{D(y_\infty - y_0)}{C} = \alpha \frac{D}{C}(1 - \xi)H, \tag{8}$$

where $\alpha \leq 1$ quantifies the final degree of segregation ($\alpha \simeq 0.79$ for our numerical flows, Figure 5).

We have little constraints on the form of the effective lift force during the segregation of a granular layer, beside the observation that segregation is driven by shear. Moreover, the presence of gravity is clearly a key ingredient in the segregation process; we may thus expect C to depend explicitly on g. In our flow configuration, however, g and $\|\dot{\gamma}\|$ are not independent quantities, and their respective contributions cannot be unambiguously disentangled. Since we are interested in connecting segregation to flow dynamics, we chose $\|\dot{\gamma}\|$ rather than g as typical time-scale for our systems. From purely dimensional considerations, a possible dependence is thus

$$C \propto \rho d_L^3 \|\dot{\gamma}\|^2. \tag{9}$$

Large shear also increases diffusive motion of the grains, hence limiting segregation: therefore C should not be a purely increasing function of the shear rate. For instance, a proposition could be: $C \propto \rho d_L^3 \|\dot{\gamma}\|^2 e^{(-\|\dot{\gamma}\|/\gamma_0)}$ where γ_0 is a characteristic value of the shear rate for which diffusion starts hindering segregation. However, for the moderate values of the shear rate simulated in the present work, we will assume that the expression (9) is an acceptable description.

The drag force experienced by an intruder moving in a granular packing is comparatively easier to investigate experimentally, and several studies (using static granular beds or fluidized ones) have been carried out to identify its form.[17,33,34] Beside a linear dependence on the velocity, it was shown to be proportional to the frictional force felt by the moving intruder. Therefore, the relevant time scale to describe the drag function is set by gravity. We propose the following form for the drag function D:

$$D \propto \mu \rho g^{1/2} d_L^{3/2}. \tag{10}$$

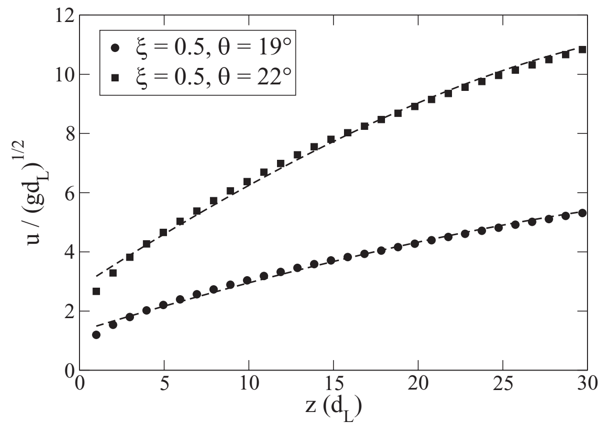

FIG. 6. Examples of velocity profiles for $\xi = 0.5$ and $\theta = 19°$ and $\theta = 22°$ averaged over the duration of the segregation process (i.e., 3τ). The dotted lines show the corresponding classical Bagnold scaling: $u(z) = A\sqrt{g}/d_L(H^{\frac{3}{2}} - (H-z)^{\frac{3}{2}}) + u_0$.

As for the lift function C, the typical length scale adopted to describe the drag function D is the mean grain diameter d_L, rather than the system thickness H. This means that we do not describe explicitly the possible dependence of the lift force on the mean pressure. This again derives from the flow configuration; an extended discussion on this specific aspect ensues in Sec. V.

Following these simple assumptions, and supposing moderate shear, we can make a prediction for the typical time scale of segregation:

$$\bar{\tau} \propto \mu \frac{y_\infty - y_0}{d_L} \|\bar{\dot{\gamma}}\|^{-2} = \mu\,\alpha(1-\xi)\frac{H}{d_L}\|\bar{\dot{\gamma}}\|^{-2}, \tag{11}$$

where $\bar{\tau} = \tau/\sqrt{d_L/g}$ and $\|\bar{\dot{\gamma}}\| = \|\dot{\gamma}\|/\sqrt{g/d_L}$.

To test the prediction against the simulations behavior, we need to evaluate the mean shear rate during the segregation process. Therefore, the mean velocity profile is computed over a duration of 3τ, such that $(y_G - y_0)/(y_\infty - y0) = 95\%$. Example profiles are shown in Figure 6: in spite of the segregation happening, it is consistent with the classical Bagnold scaling: $u(z) - u(0) \simeq A\sqrt{g}(H^{\frac{3}{2}} - (H-z)^{\frac{3}{2}})/d_L$.[35] Accordingly, the mean shear rate is given by $\langle\|\dot{\gamma}\|\rangle \simeq \frac{5}{3}(\langle u\rangle - \langle u_0\rangle)/H$, where $\langle u\rangle$ is the mean flow velocity averaged in space over the flow thickness H and in time over the duration 3τ, and $\langle u_0\rangle$ is the bottom velocity (given by the grains flowing at a height smaller than $1d_L$ from the bottom) averaged in time over the duration 3τ. Because both segregation and flow dynamics may cause variations in the compaction of the granular packing, the thickness of the flow used to evaluate the shear rate is also averaged in time over 3τ, rather than simply taken equal to the initial packing thickness. Considering simulation series 1 (i.e., varying ξ for a fixed slope $\theta = 18°$) and simulation series 3, 4, 5, and 6 (i.e., varying θ for ξ alternatively fixed to 0.16, 0.34, 0.50, and 0.67) we compute the mean shear rate $\|\dot{\gamma}\|$, and relate it to the time-scale τ in Figure 7. The data points collapse onto a single curve corresponding to the following scaling:

$$\bar{\tau} \simeq \frac{y_\infty - y_0}{d_L}\left(\|\bar{\dot{\gamma}}\|^{-2} + 75\right), \tag{12}$$

$$\simeq 0.789(1-\xi)\frac{H}{d_L}\left(\|\bar{\dot{\gamma}}\|^{-2} + 75\right), \tag{13}$$

where $\bar{\tau} = \tau/\sqrt{d_L/g}$ and $\|\bar{\dot{\gamma}}\| = \|\dot{\gamma}\|/\sqrt{g/d_L}$. The general behavior of the numerical flows is thus compatible with the prediction (11), provided that the possible variations of μ induced by the variations of ξ are small compared to the variations of ξ and $\|\dot{\gamma}\|$. The existence of an offset which sets a lower bound value for the segregation time scale was not predicted by the model; this offset implies that segregation cannot occur during a time interval shorter than $75\sqrt{d_L/g}$. This can be compared with the typical time needed for a small grain to percolate through a loose bed of large grains proceeding by successive jumps from one layer to the other: if that single bead was to fall

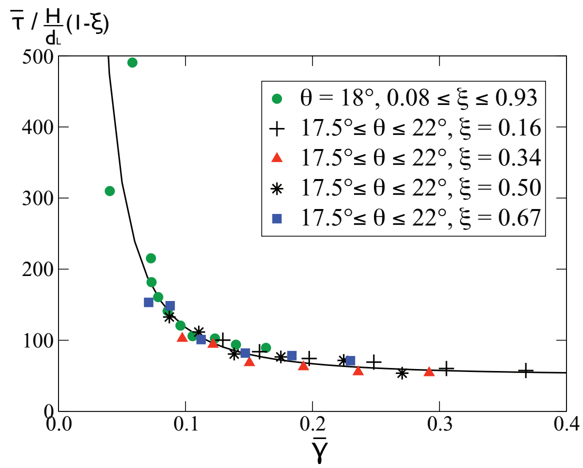

FIG. 7. The normalized typical time-scale of segregation $\bar{\tau}/\frac{H}{d_L}(1-\xi)$ as a function of the normalized shear rate $\|\bar{\dot{\gamma}}\|$ for simulation series 1, 3, 4, 5, and 6. The plain line shows $(1/\|\bar{\dot{\gamma}}\|^2 + 75)$.

down $H \simeq 22$ rows of large beads one after the other, without accelerating, then it would take 22 times the elementary fall duration $\sqrt{d_L/g}$, hence $22\sqrt{d_L/g}$. The existence of an offset for τ may be related to a similar mechanism: while shear deformation allows large and small grains to explore the space, a small grains still need to jump down a finite number of layers of large grains within successive time intervals each scaling like $\sqrt{d_L/g}$.

V. DISCUSSION

Using a discrete simulation method, we simulate numerical two-dimensional bi-disperse chute flows formed of a layer of larger grains overlaid by a layer of smaller grains, and analyze their evolution for different slopes and different volume fraction of large beads. As size segregation occurs, the position of the centre of mass of the large beads is shown to raise exponentially with time with a typical time scale decreasing with the volume fraction of large beads. Exponential evolution for grain size segregation was already observed experimentally by Golick and Daniels in Ref. 11 in a Couette cell configuration. Because these authors make a qualitative distinction between mixing (i.e., early stage of the segregation process) and separation of the grains (i.e., following stage of the segregation process), while we consider it to be a single phenomenon, their evaluation of the typical segregation time, excluding mixing, is necessarily shorter than our estimation, which includes mixing. Moreover, rather than measuring the actual position of the large grains, they measure the volume of the packing from which they infer segregation, which is likely to differ from our measurements (note that in our unconfined flow configuration, we do not observe dilation as a result of segregation). Finally, the experimental results were obtained in 3D. In spite of these differences, it is interesting to compare quantitatively the ratio of the typical time scale for segregation to the inverse of the shear rate in both studies. While data in Ref. 11 show $\tau/\|\dot{\gamma}\|^{-1} \simeq 60$ for $\xi = 0.5$ and $d_L/d_S = 2$, we find $\tau/\|\dot{\gamma}\|^{-1} \simeq 150$. Considering that a 3D flow is expected to be more efficient in segregating than a 2D flow, and in view of the differences in the measurements performed, these two results seem to be reasonably consistent.

In this paper, we show that a simple Lagrangian description of the dynamics of the phase of large grains in terms of lift and drag forces allows for the recovery of the exponential time dependence of the segregation phenomena. A similar description was proposed in Ref. 9 (in an Eulerian framework), however, a different mechanism is invoked to explain the physical origin of the lift force: the pressure screening of the smaller grains. Accordingly, the larger grains are submitted to a larger pressure gradient than hydrostatic, and rise. In other words, while our model assumes a lift function scaling as the shear rate, the lift function in Ref. 9 scales as the gravity. The result of this assumption is that the segregation velocity is not implicitly related to the flow dynamics. As mentioned in Sec. IV, shear rate and gravity cannot be independently varied in the chute flow configuration. Indeed, in the simpler mono-disperse chute flow case, it can be shown that $\|\dot{\gamma}\|$ increases like $(\sqrt{P/\rho})/d \simeq (\sqrt{gH})/d$, where d is the mean grain diameter.[36] The bi-disperse chute flows simulated here obey the same behavior, exhibiting a velocity profile compatible with the Bagnold scaling (Figure 6). Hence, one cannot unambiguously discriminate between pressure and shear rate in the expression of lift and drag forces for these systems. However, considering that the slope interval explored in our simulations allows to increase the shear rate by a factor 8, and the pressure by a factor 1.03 only, the former seems indeed to be the relevant ingredient here. Nevertheless, it would be interesting to investigate how the different partial stress tensors in a bi-phasic flows may be affected by the flow dynamics.

Another way of varying the pressure condition is to vary the flow height H, which was not explicitly considered when making predictions for the form of the lift and drag forces applied to the large grains. A first reason is that for the sake of simplicity (trying to keep the number of parameters characterizing the mean flow to a minimum), all the numerical flows considered here exhibit the same thickness H (variations due to different compactions being small). A more fundamental reason is that in the flow configuration considered here, as already discussed, shear rate and flow height cannot be varied independently. A more general model would require independent variations of both quantities (as in the Couette cell device used by Ref. 11).

The chute flow however forms a paradigm configuration to study segregation in rapid granular flows. It exhibits a very robust behavior, whereby segregation progresses exponentially with time, with a typical time scale which depends on both the volume fraction of large grains and the flow mean shear rate. A simple model balancing an effective lift force and an effective drag force applied to the centre of mass of the large grains leads to the recovery of the exponential behavior. Relating the two forces to the shear rate based on dimensional arguments and experimental findings, the model yields successful prediction of the segregation time-scale. This prediction forms a framework to understand the relation between segregation and flow dynamics in which other dependences should be tested, particularly the effect of the grain size ratio d_L/d_S. In this respect, the importance of the grain size distribution around the mean value for each grain species was demonstrated in this study. A next important step is to understand how segregation affects the flow characteristics; this will be the subject of future work.

ACKNOWLEDGMENTS

The authors thank C. G. Johnson for interesting comments on this work. This work was supported by the FP7 European Grant IEF No. 297843.

[1] J. Bridgewater, W. S. Foo, and D. J. Stephens, "Particle mixing and segregation in failure zones - Theory and experiment," Powder Technol. **41**, 147–158 (1985).
[2] S. B. Savage and C. K. K. Lun, "Particle size segregation in inclined chute flow of dry cohesionless granular solids," J. Fluid Mech. **189**, 311–335 (1988).
[3] D. M. Powell, "Patterns and processes of sediment sorting in gravel-bed rivers," Prog. Phys. Geogr. **22**(1), 1–32 (1998).
[4] P. Frey and M. Church, "How river beds move," Science **325**, 1509–1510 (2009).
[5] G. Félix and N. Thomas, "Relation between dry granular flow regimes and morphology of deposits: formation of levées in pyroclastic deposits," Earth Planet. Sci. Lett. **221**, 197–213 (2004).
[6] P. J. Rowley, P. Kokelaar, M. Menzies, and D. Waltham, "Shear-derived mixing in dense granular flows," J. Sedimentary Res. **81**, 874–884 (2011).
[7] C. G. Johnson, B. P. Kokelaar, R. M. Iverson, M. Logan, R. G. LaHusen, and J. M. N. T. Gray, "Grain-size segregation and levee formation in geophysical mass flows," J. Geophys. Res. **117**, F01032, doi:10.1029/2011JF002185 (2012).
[8] A. Kudrolli, "Size separation in vibrated granular matter," Rep. Prog. Phys. **67**, 209–247 (2004).
[9] J. M. N. T. Gray and A. R. Thornton, "A theory for particle size segregation in shallow granular free-surface flows," Proc. R. Soc. A **461**, 1447–1473 (2005).
[10] C. Goujon, B. Dalloz-Dubrujeaud, and N. Thomas, "Bidisperse granular avalanches on inclined planes: A rich variety of behaviors," Eur. Phys. J. E **23**, 199–215 (2007).
[11] L. A. Golick and K. E. Daniels, "Mixing and segregation rates in sheared granular materials," Phys. Rev. E **80**, 042301 (2009).
[12] F. Moro, T. Faug, H. Bellot, and F. Ousset, "Large mobility of dry snow avalanches: Insights from small-scale laboratory tests on granular avalanches of bidisperse materials," Cold Reg. Sci. Technol. **62**, 55–66 (2010).

[13] J. M. N. T. Gray and B. P. Kokelaar, "Large particle segregation, transport and accumulation in granular free-surface flows," J. Fluid Mech. **652**, 105–137 (2010).
[14] L. B. H. May, L. A. Golick, K. C. Phillips, M. Shearer, and K. E. Daniels, "Shear-driven size segregation of granular materials: Modeling and experiment," Phys. Rev. E **81**, 051301 (2010).
[15] C. Meruane, A. Tamburrino, and O. Roche, "Dynamics of dense granular flows of small-and-large-grain mixtures in an ambient fluid," Phys. Rev. E **86**, 026311 (2012).
[16] B. Marks, P. Rognon, and I. Einav, "Grainsize dynamics of polydisperse granular segregation down inclined planes," J. Fluid Mech. **690**, 499–511 (2012).
[17] F. Guillard, Y. Forterre, and O. Pouliquen, "Depth-independent drag force induced by stirring in granular media," Phys. Rev. Lett. **110**, 138303 (2013).
[18] J. C. Phillips, A. J. Hogg, R. R. Kerswell, and N. H. Thomas, "Enhanced mobility of granular mixtures of fine and coarse particles," Earth Planet. Sci. Lett. **246**, 466–480 (2006).
[19] E. Linares-Guerrero, C. Goujon, and R. Zenit, "Increased mobility of bidisperse granular avalanches," J. Fluid Mech. **593**, 475–504 (2007).
[20] P. G. Rognon, J.-N. Roux, M. Naaim, and F. Chevoir, "Dense flows of bidisperse assemblies of disks down an inclined plane," Phys. Fluids **19**, 058101 (2007).
[21] B. Yohannes and K. M. Hill, "Rheology of dense granular mixtures: Particle-size distributions, boundary conditions, and collisional time scales," Phys. Rev. E **82**, 061301 (2010).
[22] A. Tripathi and D. V. Khakhar, "Rheology of binary granular mixtures in the dense flow regime," Phys. Fluids **23**, 113302 (2011).
[23] O. Pouliquen, J. Delour, and S. B. Savage, "Fingering in granular chute flows," Nature (London) **386**, 816–817 (1997).
[24] M. J. Woodhouse, A. R. Thornton, C. G. Johnson, B. P. Kokelaar, and J. M. N. T. Gray, "Segregation-induced fingering instabilities in granular free surface flows," J. Fluid Mech. **709**, 543–580 (2012).
[25] J. M. N. T. Gray and V. A. Chugunov, "Particle-size segregation and diffusive remixing in shallow granular avalanches," J. Fluid Mech. **569**, 365–398 (2006).
[26] I. Zuriguel, J. M. N. T. Gray, J. Peixinho, and T. Mullin, "Pattern selection by a granular wave in a rotating drum," Phys. Rev. E **73**, 061302 (2006).
[27] A. R. Thornton, T. Weinhart, S. Luding, and O. Bokhove, "Modeling of particle size segregation: Calibration using the discrete particle method," Int. J. Mod. Phys. C **23**, 1240014 (2012).
[28] M. Jean and J.-J. Moreau, "Unilaterality and dry friction in the dynamics of rigid bodies collections," in *Proceedings of Contact Mechanics International Symposium*, edited by A. Curnier (Presses Polytechniques et Universitaires Romandes, Lausanne, 1992), pp. 31–48.
[29] C. Voivret, F. Radjai, J.-Y. Delenne, and M. S. El Youssoufi, "Multiscale force networks in highly polydisperse granular media," Phys. Rev. Lett. **102**, 178001 (2009).
[30] K. Wieghardt, "Experiments in granular flow," Annu. Rev. Fluid Mech. **7**, 89–113 (1975).
[31] O. Zik, J. Stavans, and Y. Rabin, "Mobility of a sphere in vibrated granular media," Europhys. Lett. **17**(4), 315–319 (1992).
[32] G. I. Tardos, M. I. Khan, and D. G. Schaeffer, "Forces on a slowly rotating, rough cylinder in a Couette device containing a dry, frictional powder," Phys. Fluids **10**, 335 (1998).
[33] R. Albert, M. A. Pfeifer, A.-L. Barabási, and P. Schiffer, "Slow drag in a granular medium," Phys. Rev. Lett. **82**, 205–208 (1999).
[34] K. A. Reddy, Y. Forterre, and O. Pouliquen, "Evidence of mechanically activated processes in slow granular flows," Phys. Rev. Lett. **106**, 108301 (2011).
[35] R. G. Bagnold, "Experiments of gravity-free dispersion of large solid spheres in a Newtonian fluid under shear," Proc. R. Soc. London, Ser. A **225**, 49 (1954).
[36] GDR Midi, "On dense granular flows," Eur. Phys. J. E **14**(4), 341–365 (2004).